Program Digest, 2019 IEEE International Ultrasonics Symposium (IUS)
Glasgow, Scotland, October 6-9, 2019

Assessment of Side Lobe Estimation Accuracy Using Side Lobe Free Image

Mok Kun Jeong[1] and Sung Jae Kwon[2]
[1]Department of Electronic Engineering
[2]Division of Human IT Convergence Engineering
Daejin University
Pocheon, Republic of Korea
jmk@daejin.ac.kr

Min Joo Choi
Department of Medicine
School of Medicine
Jeju National University
Jeju, Republic of Korea

Abstract*—In order to effectively suppress side lobes in ultrasound imaging, it is necessary to quantify the signal amplitude due to side lobes at imaging points. The received channel data before receive beamforming are modeled as a sum of sinusoids having different spatial frequencies depending on the angle incident on a receiving array. In the signal constituting the channel data, the signal due to the main lobe has a DC frequency, whereas the signal due to the side lobe has a spatial frequency that is approximately proportional to the incident angle. Taking the Fourier transform of the received channel data after zero padding, we can accurately estimate side lobes. In computer simulation of ultrasound images, we generate ultrasonic echoes returned from random scatterers. Because we already know the position of all reflectors, we can separate the signals reflected due to the main and side lobes so that the true side lobe level at each imaging point can be computed accurately. The main lobe image can be used as a gold standard for assessing a side lobe suppression filter. The true and estimated side lobes can be used in side lobe suppression filtering of ultrasound images. We obtained the conventional, true side lobe, and estimated side lobe images for an object containing a wire and a cyst using computer simulation in a 64 channel focusing system with a 5 MHz linear array transducer. In the hypoechoic cyst, the estimated side lobe is almost the same as the true side lobe. We confirmed that the estimated side lobe can effectively be used in side lobe suppression filtering. Therefore, it is feasible to quantitatively estimate side lobes from the channel data, and improve the performance of the side lobe suppression filter in ultrasound imaging.

Keywords—side lobe estimation; side lobe free image; spatial frequency; ultrasound image

I. Introduction

The image resolution in medical ultrasound imaging is determined by the main lobe width of ultrasound field, and both signal-to-noise ratio and contrast-to-noise ratio depend on side lobe characteristics. A medical ultrasound imaging system uses an array transducer to focus the transmit and receive signals and improve ultrasound field characteristics by applying signal processing techniques [1]. A variety of signal processing techniques have been developed to reduce side lobes in receive focusing, including apodization that multiplies the received channel data with a weight such as the Hamming window [2].

Minimum variance beamforming methods are also used in ultrasound imaging, which multiply the received channel data at every imaging point with an optimum set of weights according to ultrasound field characteristics [3]–[5]. Methods of determining weights using the coherence of the received channel data to suppress side lobes are investigated [6]–[8]. These methods improve image quality using the qualitative characteristics of side lobes. Quantitative estimation of side lobe levels may lead to image improvement in many ways. Methods of estimating side lobe levels in the received channel data using Fourier transform and side lobe waveforms directly were reported [9], [10].

In this paper, we estimate the side lobe waveform using the received channel data. Using computer simulation, we separate the main and side lobes and compute their magnitudes. We compared in magnitude the estimated side lobe with the true side lobe computed from ultrasound field characteristics. The estimated and true side lobes are used in side lobe suppression filtering, and the results are compared.

II. Side Lobe Estimation

The receive focusing block in an ultrasound imaging system compensates for different arrival times to align echoes in time. Since an ultrasound signal can be modeled as a sine wave pulse, the received channel data after focusing can be modeled as a sinusoidal wave whose spatial frequency is dependent on the incident angle θ on an array transducer. The spatial frequency of the side lobe is given by

$$f = \frac{D}{\lambda}\sin\theta\,, \qquad (1)$$

where D is the total aperture size and λ is the wavelength of the center frequency [9], [10]. Since the echoes returned from an imaging point of interest have an incidence angle of 0°, the spatial frequency of the received channel data is 0 Hz. Echoes from null directions in the lateral field response form a sine wave whose spatial frequency is an integer.

Fig. 1 shows a waveform of the received channel data when echoes are coming from the first side lobe position. Since side lobe components, which have an adverse effect on image quality, have a spatial frequency of an integer plus a half, they do not have an integer spatial frequency when Fourier transformed. However, taking the Fourier transform of the received channel data after zero padding results in the side lobe components having an integer spatial frequency as shown in Fig. 2 [11]. Using this property, we can estimate side lobe waveforms from the received channel data according to individual spatial frequencies. By estimating side lobe levels at imaging points, we obtain an estimated side lobe image.

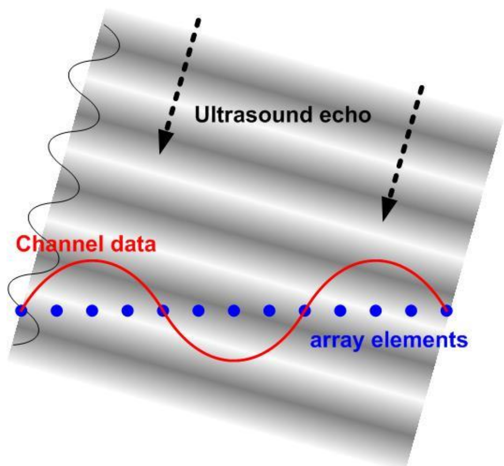

Fig. 1. Modeling of the received channel data as a sine wave for a specific incident direction corresponding to the first side lobe position.

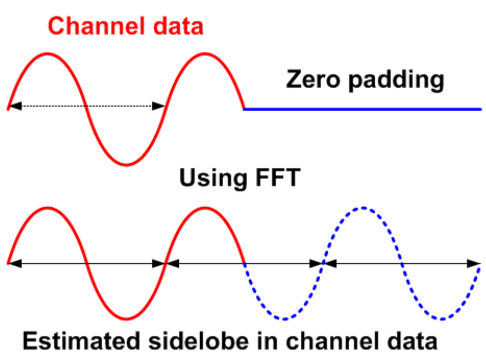

Fig. 2. Estimation of side lobe after zero padding the received channel data.

III. Side Lobe Free Imaging

In a transmit and receive focusing system, the signal at an imaging point is obtained by compensating for transmit and receive focusing time delays when ultrasonic signals fired from transmit elements are reflected from the point and arrive at receive elements. In computer simulation, for the case of a 64 channel system, at each imaging point, the echoes are added up for 4,096 combinations of the transmit and receive transducer elements.

Once the specifications of a focusing system have been determined, the ultrasound field characteristics can also be identified. As shown in Fig. 3, when a scatterer is inside (propagation path indicated in solid line) and outside (dashed line) the main lobe region of the ultrasound field, the echoes can be separately computed to construct images [12]. The images constructed when the scatterer is inside and outside the main lobe region of ultrasound field is termed the main lobe image and the true side lobe image, respectively. The main lobe width is defined as the width between the left and right first nulls of the ultrasound field in the lateral direction.

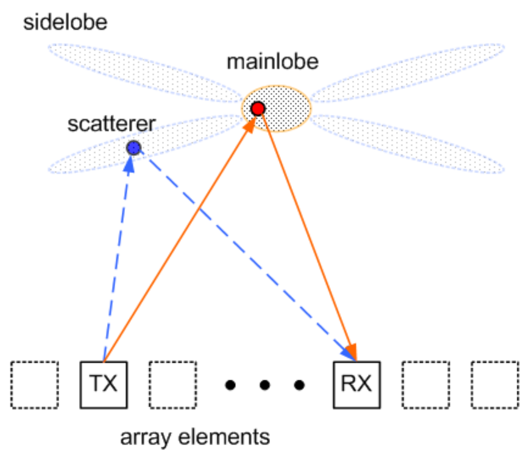

Fig. 3. Separation of propagation paths by scatterer positions.

IV. Computer Simulation

A point spread function was obtained by computer simulation on a point target at a depth of 37.5 mm in a 64 channel linear array transducer system. The center frequency was 5 MHz, and the element width was 0.3 mm. A three cycle Gaussian pulse was used, and the transmit focal depth was 30 mm. Fig. 4 shows the main and side lobe images of the point target, where (a) is the point spread function, (b) is the main lobe image, (c) is the true side lobe image, and (d) is the estimated side lobe image. All the images are logarithmically compressed over a range of 60 dB. The true and estimated side lobes are similar in both level and shape.

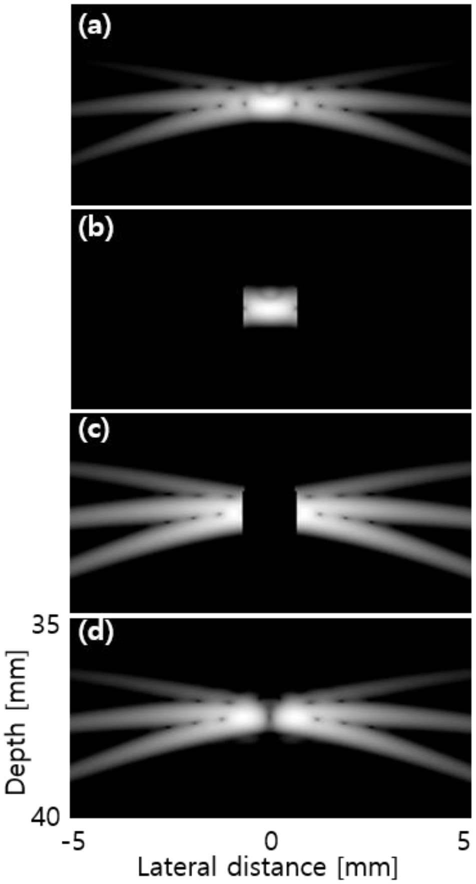

Fig. 4. Main and side lobe images of a point target: (a) point spread function, (b) main lobe image, (c) true side lobe image, and (d) estimated side lobe image.

We constructed speckled images of two cysts of diameter 4 mm that have a reflectivity of –20 dB and –30 dB relative to the background. Fig. 5 shows the main lobe, side lobe, and filtered images, where (a) is the conventional cyst image, (b) is the main lobe image, (c) is the true side lobe, and (d) is the estimated side lobe. All the images are logarithmically compressed over a 60 dB range. The difference in contrast between the two cysts in Fig. 5(b) can clearly be seen. Inside the cysts marked with white arrows, the true and estimated side lobes exhibit a similar pattern. Since the side lobe level is inversely proportional to the image quality, we adopted the magnitude of the estimated side lobe as a quality factor. Accordingly, we define a side suppression filter as follows:

$$B_{filtered} = \left(\frac{1}{1+\gamma\left(\dfrac{QF_P}{B_{pixel}}\right)} \right) \cdot B_{pixel}\,, \tag{2}$$

where B_{pixel} is the image brightness, γ is an empirically determined scale factor, and QF_P is the quality factor based on the side lobe level at each imaging point [13]. Fig. 5(e) and (f) are the images filtered with QF_P computed from the true and estimated side lobes, respectively. γ was set to 2. First removing side lobes from images and then filtering using (2) yields the following:

$$B_{filtered} = \left(\frac{1}{1+\gamma\left(\dfrac{QF_P}{B_{pixel}}\right)} \right) \cdot \left(B_{pixel} - QF_P \right). \tag{3}$$

Filtering using (3) with QF_P computed from the estimated side lobe, we obtain the image of Fig. 5(g) where the contrast inside the two cysts is similar to that of the main lobe image. Fig. 5(g) is most similar to Fig. 5(b) in terms of the background speckle pattern.

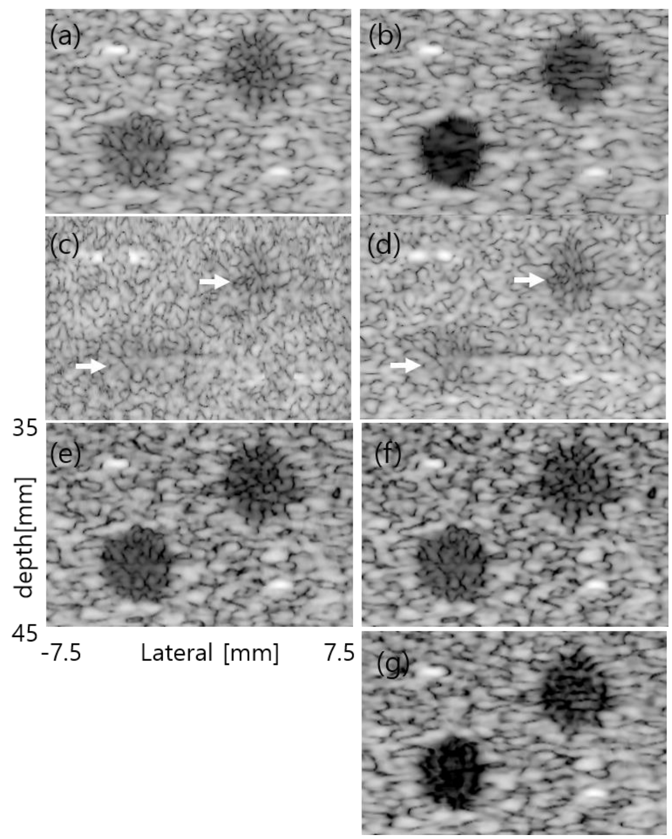

Fig. 5. Various images of two cysts: (a) conventional cyst image, (b) main lobe image (c) true side lobe, (d) estimated side lobe, (e) filtered image using true side lobe, (f) filtered image using estimated side lobe, and (g) another filtered image using estimated side lobe.

V. Conclusion

We estimated side lobes by taking the Fourier transform of the zero-padded channel data. The estimated side lobes exhibited a similar pattern to the true side lobes theoretically estimated. Having no side lobes at all, the main lobe image can be used as a standard for assessing the efficacy of filtering out side lobes. It is confirmed by comparing the output image of side lobe filtering using the estimated side lobe with the main lobe image that side lobes can effectively be suppressed.

REFERENCES

[1] A. Macovski, Medical Imaging Systems. Englewood Cliffs, N.J.: Prentice-Hall, 1983.

[2] M. Fink, W. A. Kuperman, J. P. Montagner, and A. Tourin, Imaging of Complex Media with Acoustic and Seismic Waves. Berlin: Springer-Verlag, 2002.

[3] B. Van Veen and K. M. Buckley, “Beamforming: a versatile approach to spatial filtering,” IEEE ASSP Mag., vol. 5, no. 2, pp. 4–24, Apr. 1988.

[4] F. Viola and W. F. Walker, “Adaptive signal processing in medical ultrasound beamforming,” in Proc. IEEE Ultrason. Symp., 2005, pp. 1980–1983.

[5] K. Kim, S. Park, J. Kim, S. B. Park, and M. Bae, “A fast minimum variance beamforming method using principal component analysis,” IEEE Trans. Ultrason. Ferroelectr. Freq. Control, vol. 61, no. 6, pp. 930-945, Jun. 2014.

[6] K. W. Hollman, K. W. Rigby, and M. O’Donnell, “Coherence factor of speckle from a multi-row probe,” in Proc. IEEE Ultrason. Symp., 1999, pp. 1257–1260.

[7] M. A. Lediju, G. E. Trahey, B. C. Byram, and J. J. Dahl, “Short-lag spatial coherence of backscattered echoes: imaging characteristics,” IEEE Trans. Ultrason. Ferroelectr. Freq. Control, vol. 58, no. 7, pp. 1377–1388, Jul. 2011.

[8] J. Camacho, M. Parrilla, and C. Fritsch, “Phase coherence imaging,” IEEE Trans. Ultrason. Ferroelectr. Freq. Control, vol. 56, no. 5, pp. 958–974, May 2009.

[9] M. K. Jeong, “A Fourier transform-based sidelobe reduction method in ultrasound imaging,” IEEE Trans. Ultrason. Ferroelectr. Freq. Control, vol. 47, no. 3, pp. 759–763, May 2000.

[10] M. K. Jeong and S. J. Kwon, “Estimation of side lobes in ultrasound imaging systems,” Biomed. Eng. Lett., vol. 5, no. 3, pp. 229–339, 2015.

[11] M. K. Jeong and S. J. Kwon, “A novel side lobe estimation method in medical ultrasound imaging systems,” in Proc. IEEE Ultrasonics Symp, 2015.

[12] M. K. Jeong and S. J. Kwon, “Side lobe free medical ultrasonic imaging with application to assessing side lobe suppression filter,” Biomed. Eng. Lett., vol. 8, no. 4, pp. 355–364, 2018.

[13] S. J. Kwon and M. K. Jeong, “Estimation and suppression of side lobes in medical ultrasound imaging systems,” Biomed. Eng. Lett., vol. 7, no. 1, pp. 31–43, 2017.